Extragenic Suppressors of Paralyzed Flagellar Mutations in *Chlamydomonas reinhardtii* Identify Loci That Alter the Inner Dynein Arms

Mary E. Porter,*‡ Joy Power,‡ and Susan K. Dutcher‡

*Department of Cell Biology and Neuroanatomy, University of Minnesota Medical School, Minneapolis, Minnesota 55455; and ‡Department of Molecular, Cellular, and Developmental Biology, University of Colorado at Boulder, Boulder, Colorado 80309-0347

Abstract. We have analyzed extragenic suppressors of paralyzed flagella mutations in *Chlamydomonas reinhardtii* in an effort to identify new dynein mutations. A temperature-sensitive allele of the *PF16* locus was mutagenized and then screened for revertants that could swim at the restrictive temperature (Dutcher et al. 1984. *J. Cell Biol.* 98:229–236). In backcrosses of one of the revertant strains to wild-type, we recovered both the original *pf16* mutation and a second, unlinked suppressor mutation with its own flagellar phenotype. This mutation has been identified by both recombination and complementation tests as a new allele of the previously uncharacterized *PF9* locus on linkage group XII/XIII. SDS-PAGE analysis of isolated flagellar axonemes and dynein extracts has demonstrated that the *pf9* strains are missing four polypeptides that form the I1 inner arm dynein subunit. The primary effect of the loss of the I1 subunit is a decrease in the forward swimming velocity due to a change in the flagellar waveform. Both the flagellar beat frequency and the axonemal ATPase activity are nearly wild-type. Examination of axonemes by thin section electron microscopy and image averaging methods reveals that a specific domain of the inner arm complex is missing in the *pf9* mutant strains (see accompanying paper by Mastronarde et al.). When combined with other flagellar defects, the loss of the I1 subunit has synergistic effects on both flagellar assembly and flagellar motility. These synthetic phenotypes provide a screen for new suppressor mutations in other loci. Using this approach, we have identified the first interactive suppressors of a dynein arm mutation and an unusual bypass suppressor mutation.

THE dynein ATPases are large and complex multisubunit enzymes that provide the force for a variety of microtubule based movements inside cells (reviewed in Gibbons, 1988; Porter and Johnson, 1989). In cilia and flagella, at least nine different dynein heavy chains have been described; these and other polypeptides are arranged into at least four different dynein arm subunits (Piperno et al., 1990). The presence of these multiple dynein isoforms within the axoneme provides the cell with several different potential mechanisms for affecting the flagellar waveform, but how the activity of the different dyneins is coordinated is not well understood. Both the inner and outer dynein arms can drive the sliding movements between adjacent outer doublet microtubules that serve as the basis for ciliary movement. However, study of flagellar mutations in *Chlamydomonas* has revealed that the different dynein arms have different functions in the generation of flagellar motility. For instance, mutant strains that lack outer arm polypeptides swim with a reduced flagellar beat frequency, whereas mutant strains that lack subsets of inner arm polypeptides swim with an altered flagellar waveform (Brokaw and Kamiya, 1987).

The flagellar dyneins also play an important but poorly understood role in modifying the flagellar waveform in response to signals from other axonemal components. Mutations that disrupt the radial spokes or central pair structures (e.g., *pf17* or *pf16*) generally lead to flagellar paralysis, even though the motor activity of the dynein arm is apparently normal as assayed by sliding disintegration tests (Witman et al., 1978). The discovery of extragenic suppressors (*sup-pf-1*, *sup-pf-2*, *sup-pf-3*, *sup-pf-4*, *pf2*, and *pf3*) that restored some degree of flagellar motility without repair of the original central pair or radial spoke defects revealed the existence of a second control system in the axoneme that can alter dynein activity (Huang et al., 1982*b*). The axonemal location of these suppressor-related control systems was not identified, with the exception of a single suppressor locus (*sup-pf-1*) that appeared to modify one of the outer dynein arm polypeptides. Subsequent analysis of the *pf2* and *pf3* mutant strains has suggested that they may exert their suppressor activity by modifying the inner dynein arms (Brokaw and Kamiya, 1987; Luck and Piperno, 1989).

These results indicated that these bypass suppressors can reveal control elements in the axoneme that are both intrinsic and extrinsic to dynein arms. It seemed reasonable to sup-

© The Rockefeller University Press, 0021-9525/92/09/1163/14 $2.00

pose that further study of this class of mutation would provide new insights into the mechanism of flagellar motility. Following this strategy, we have identified a new bypass suppressor that restores motility to a central pair defective strain, and we have undertaken a detailed characterization of this suppressor strain. Our results indicate that the suppressor is one of several mutant alleles at the *PF9* locus. Mutations at this locus affect a subset of inner dynein arm polypeptides that form the I1 inner arm subunit. Examination of recombinant strains containing both *pf9-2* and other flagellar mutations indicates that the loss of the I1 subunit can have pleiotropic effects on both flagellar motility and flagellar assembly. We have used these double mutant phenotypes as a tool for identifying the network of loci that mediate the assembly of inner dynein arms.

Concurrent with our study, reports on other dynein mutations have indicated that the structure of the inner dynein arm is very complex. Images obtained by quick-freeze deep etch techniques have suggested that the inner arms form a triplet repeat of a three-headed arm and two double-headed arms every 96 nm (Goodenough and Heuser, 1989). Analysis of flagellar mutations that are missing distinct subsets of inner arm dynein polypeptides supports the notion of a triplet repeat. Discrete gaps in inner arm density are observed at regular intervals in longitudinal thin sections of isolated axonemes (Piperno et al., 1990). On the other hand, a recent analysis of similar mutant strains from cross-sections has been interpreted as two distinct rows of inner dynein arms (Kamiya et al., 1991). We have used a similar approach with improved image averaging techniques to examine the mutants described in this report and several related inner arm dynein mutants. These results are described in the accompanying paper (Mastronarde et al., 1992).

Materials and Methods

Mutant Strains

All strains were derived from stocks maintained in our laboratory except as noted. The strains *lf2*, *oda4*, *oda6*, *oda9*, *pf2*, *pf9-1*, and *pf28* were obtained from the *Chlamydomonas* Genetics Center (Department of Botany, Duke University, Durham NC). *Ida1* (*ida98*) and *ida4* (*idb*) were generously provided by Dr. R. Kamiya (Nagoya University, Nagoya, Japan). The phenotypes of motility mutations (*ida*, *lf*, *oda*, *pf*, etc.) were scored by phase contrast microscopy.

Cell Culture

Cells were maintained as vegetatively growing cultures at 21°C on rich medium containing sodium acetate, as described by Sager and Granick (1953) and modified by Holmes and Dutcher (1989). Cultures of gametic cells were obtained by transferring strains to a low-sulphate medium for 5–7 d. All solid media contained Bacto agar (Difco Laboratories, Detroit, Michigan) that was washed five times with Milli-Q filtered water and air dried before use. The medium for large scale (>5 liters) liquid culture was supplemented with additional potassium phosphate as described by Witman (1986). The markers *arg2* (Eversole, 1956) and *arg7-2* (Loppes, 1969) were scored on rich medium with one-tenth the normal concentration of ammonium nitrate and 100 μg/ml arginine-HCl.

Genetic Analysis

New mutations were mapped to their genetic loci by recombination analysis of tetrad progeny using standard techniques (Levine and Ebersold, 1960; Harris, 1989). Dominance and complementation tests were performed by constructing stable diploid cell lines (Ebersold, 1967). Each mutation was crossed into an arginine-requiring background (either *arg2* or *arg7*) and the appropriate diploid was selected on medium lacking arginine. At least six independently isolated cell lines were examined for each diploid construction, and all diploids were demonstrated to be mating type minus.

Reversion Analysis at the PF16 Locus

Revertants of the temperature-sensitive *pf16BR3* mutant strain (Dutcher et al., 1984) were obtained by ultraviolet radiation of gametic cells for 45 s (Luck et al., 1977) and then screening 20-ml liquid cultures for swimming cells at the restrictive temperature of 32°C. 48 independent revertants were isolated, and each revertant was backcrossed to the wild-type strain 137c and analyzed by standard techniques (Levine and Ebersold, 1960).

Reversion Analysis at the PF9 Locus

Revertants of the paralyzed *pf9-2 pf28* double mutant strain were induced by irradiation or chemical mutagenesis and then screened for the presence of swimming cells in liquid culture at 21°C.

Ultraviolet irradiation. Lawns of ~10^8 cells on petri plates were irradiated under a 30-W germicidal UV lamp (model G3T08; General Electric Co.) at a distance of 15 cm for 45 s. Plates were then wrapped in aluminum foil for 24 h.

Gamma irradiation. Plates of cells were exposed to gamma rays by placement in a Cs-137 source (model 143; J. L. Shepherd and Associates, Glendale, CA) with emissions of 502 R/min for 20 min.

Chemical mutagenesis was performed by treatment with ethyl methanesulfonate (EMS)[1] or diepoxybutane (DEB).

EMS treatment. 5 ml of cells at 7 × 10^5 cells/ml were treated with EMS at a concentration of 20 μl/ml for 35 min and then washed three times with 1% sodium thiosulfate in minimal medium to inactivate the EMS.

DEB treatment. 10 ml of cells at 4 × 10^6 cells/ml were treated with 0.3 ml of a 1:100 dilution of DEB for 45 min and then washed several times with fresh medium.

Mutagenized cells were then resuspended and aliquotted into 48 or 96 20-ml tubes of rich medium. After 24 h the upper 5 ml of the culture was transferred to fresh medium and held at 21°C until visible numbers of cells became apparent in the upper portion of the tube. The upper 5 ml was serially transferred at least three more times to enrich for cells that had recovered at least some ability to swim in liquid culture. 200 μl were plated from each tube onto solid medium, single colonies were picked, and their swimming phenotypes were scored by phase contrast microscopy. In general, only one revertant isolate from each tube was retained. In one case, two revertants with different phenotypes were isolated from the same tube. We also tested the background of spontaneous reversion by running a parallel screen with nonmutagenized cells: 2 × 10^6 cells were aliquotted into 96 tubes and screened in parallel with the EMS-treated cells. No spontaneous revertants were recovered under these conditions.

Motility and Flagellar Length Measurements

Altered flagellar motility was assessed by phase contrast microscopy on a Zeiss standard or Axioscop microscope using a ×40 objective and a ×10 eyepiece for a final magnification of 400. Measurements of swimming velocities were made from video recordings (BC-1000 VCR; Mitsubishi Electric Sales of America, Cypress, CA) of live cells using a C2400 Newvicon camera (Hamamatsu Photonic Systems Corporation, Bridgewater, NJ) and an Argus 10 video processor (Hamamatsu Photonic Systems Corporation) calibrated with a stage micrometer. Length measurements were made on individual flagella that had been detached by 1 mM dibucaine-HCl treatment of live cells. More detailed analysis of flagellar waveforms and flagellar beat frequencies was performed by dark-field microscopy using a stroboscopic light source (model 136; Chadwick-Helmuth, Monrovia, CA, on loan from Dr. E. D. Salmon, University of North Carolina, Chapel Hill, NC).

Protein Purification

Whole axonemes were obtained from small scale cultures of gametic cells on solid medium. The cells were resuspended in minimal medium, allowed to generate flagella for 15–30 min, and collected by centrifugation. Cells

1. *Abbreviations used in this paper*: CM, centimorgan; DEB, diepoxybutane; EMS, ethyl methanesulfonate; HMEEK buffer, 30 mM Hepes, pH 7.4, 5 mM $MgSO_4$, 1 mM EGTA, 0.1 mM EDTA, 25 mM KCl, 1 mM DTT, and 2.5 μg/ml aprotinin, leupeptin, and pepstatin; PD, parental ditype; NPD, non-parental ditype; TT, tetratype.

were washed free of debris and cell wall material by two cycles of resuspension and centrifugation in minimal medium, resuspended in 10 mM Hepes, pH 7.4, 1 mM $SrCl_2$, 4% sucrose, and 1 mM DTT, and then deflagellated by pH shock (Luck et al., 1977). The solution of deflagellated cells was then supplemented to 5 mM $MgSO_4$, 1 mM EGTA, and 2.5 μg/ml aprotinin, leupeptin, and pepstatin and centrifuged at 1,000 *g*. The supernatant containing flagella was removed and recentrifuged twice with a 20% sucrose cushion to trap any remaining cell bodies or debris. The clarified flagella were extracted with 0.1% NP-40, and axonemes were collected by centrifugation at 35,000 *g* for 60 min. The axoneme pellet was then resuspended in HMEEK buffer (30 mM Hepes, pH 7.4, 5 mM $MgSO_4$, 1 mM EGTA, 0.1 mM EDTA, 25 mM KCl, 1 mM DTT, and 2.5 μg/ml aprotinin, leupeptin, and pepstatin), split into two aliquots, and recentrifuged at 14,000 *g* to obtain parallel samples for SDS-PAGE analysis and electron microscopy.

Purified dyneins were prepared from large-scale liquid cultures of vegetative cells. These cells were collected using a Pellicon Cell Harvester (Millipore Corporation, Bedford, MA) equipped with Durapore filter cassettes, and then washed and deflagellated as described above. The final supernatant of clarified flagella was collected directly by centrifugation, resuspended in HMEEK, stripped of flagellar membranes by extraction in 1% NP-40, washed two to three times to remove the detergent, and then extracted in HMEEK containing either 5 mM ATP or 0.6 M KCl, 0.1 mM ATP, and 10 μM taxol for 30 min. The dynein-containing supernatant was collected after centrifugation at 30,000 *g* for 30 min, dialyzed against HMEEK for 2–3 h, clarified by centrifugation, loaded onto 5–20% sucrose density gradients (13 ml), and centrifuged in a SW41 rotor (Beckman Instruments) for 11 h at 39,000 rpm. Gradients were collected into 20–30 fractions and analyzed by ATPase assays and SDS-PAGE.

Biochemical Procedures

ATPase activity was measured in the presence of 0.3 M KCl, 30 mM Tris-HCl, pH 8.0, 5 mM $MgSO_4$, 0.1 mM EGTA, and 1 mM ATP. Inorganic phosphate released was determined colorimetrically by the method of Waxman and Goldberg (1982). Protein concentrations were determined by the method of Bradford (1976) using BSA as a standard.

SDS-PAGE

Because of the technical difficulties associated with resolving the multiple dynein heavy chain species, we compared our different samples with several previously characterized dynein mutants on multiple gel systems. These included the Laemmli-based buffer system (1970) using either 3–5% polyacrylamide, 2–8 M urea gradient gels (King et al., 1986), or 4–8% polyacrylamide, 3 M urea gradient gels (Mitchell and Rosenbaum, 1985), or the Neville-based buffer system (1971) using 3.2–5% polyacrylamide, 2–8 M urea gradient gels (Piperno and Luck, 1979). We have used a modification of the system described by King et al. (1986) for the figures shown here. Intermediate and light chain compositions were determined by separation of polypeptides on 5–15% polyacrylamide gels containing standard or reduced amounts of bis-acrylamide. Some samples were also analyzed by two-dimensional gel electrophoresis as described by Dutcher et al. (1984).

Nomenclature of Dynein Heavy Chains

We identify the dynein heavy chains using the nomenclature of Piperno et al. (1990) whenever possible. In general, the 1α and 1β inner arm heavy chains migrate between the β and γ outer arm heavy chains, the 2′ and 3′ inner arm heavy chains run as a broad single band (designated region 2) which comigrates with the γ heavy chain, and the 2 and 3 inner arm heavy chains run as a doublet (designated region 3) ahead of the γ heavy chain.

Electron Microscopy

Pellets of axonemes were processed for electron microscopy by fixation with 2% glutaraldehyde, 4% tannic acid (AR1764; Mallinkrodt Inc., St. Louis, MO), and 50 mM sodium phosphate, pH 6.9, for 1 h at room temperature, followed by fixation overnight in 2% glutaraldehyde and 50 mM sodium phosphate. Samples were transferred to fresh fixative, shipped by overnight express on wet ice, and then post-fixed in 1% OsO_4, rinsed in distilled H_2O, dehydrated in a graded acetone series, and embedded in Epon-Araldite. Silver gray sections (~60 nm thick) were double stained with lead citrate and uranyl acetate and examined at a magnification of 39,000 with a CM10 microscope (Philips Electronic Instruments Co., Mahwah, NJ) operating at 80 kV.

Axoneme cross-sections were selected for further study based on the presence of intact central pair microtubules and clear tubulin protofilament substructure. The methods used to compute the averages of the dynein images and compare the dynein arms from different mutant strains are described in the accompanying paper (Mastronarde et al., 1992).

Results

Isolation of a New Inner Arm Dynein Mutation by Suppressor Analysis

Mutations at the *PF16* locus alter the assembly of a subset of axonemal polypeptides associated with the C1 microtubule of the central pair. The temperature-sensitive strain *pf16BR3* swims normally at 21°C, but is paralyzed at 32°C (Dutcher et al., 1984). 48 independent revertants of the paralyzed phenotype were obtained by screening mutagenized cultures of the *pf16BR3* strain for swimmers at the restrictive temperature (see Materials and Methods). 17 of the revertants are intragenic and 31 are extragenic, based on an average of 12 tetrads for each revertant strain when backcrossed to the 137c wild-type strain. The extragenic suppressors can be divided into two groups based on their axonemal phenotypes on two-dimensional gels. 20 extragenic revertants may be interactive suppressors; they rescue the *pf16* mutation by restoring the missing central pair polypeptides. 11 of the extragenic revertants are bypass suppressors; they fail to restore the missing *pf16* polypeptides. Five of the bypass suppressors also demonstrate altered flagellar motility at the permissive temperature for *pf16BR3*. One of these bypass suppressors has a unique axonemal polypeptide phenotype and is the subject of this report.

We crossed the double mutant to wild-type cells and recovered both the original *pf16BR3* mutation and the new mutation, which has an altered flagellar waveform. We analyzed the flagellar phenotypes of the tetrad progeny from the cross of the double mutant to wild-type at both the permissive and restrictive temperatures for the *pf16BR3* mutation. At 21°C, two distinct motility phenotypes were easily distinguished by phase contrast microscopy: the rapid forward progression of wild-type cells, and a second slower pattern. At 32°C, this slower pattern segregated independently from the flagellar paralysis associated with the *pf16BR3* mutation and cosegregated with the suppressor activity (see below). More detailed analysis of the motility phenotype by comparison with other flagellar mutants indicated that the suppressor strain was similar to strains with inner arm dynein defects (Brokaw and Kamiya, 1987). The flagellar beat frequency is nearly wild-type, but forward swimming velocity of the cells is decreased, apparently because the amplitude of the flagellar waveform is reduced.

Because the suppressor mutation showed such a pronounced motility phenotype, we tested it for allelism with other flagellar mutations. Recombination analysis revealed that the suppressor mutation is tightly linked to alleles at the previously uncharacterized *PF9* locus on linkage group XIII (see Table I). The original *pf9-1* strain was identified as a paralyzed flagellar mutant that displayed abnormal motility, but no detailed description of this strain exists (Hastings et al., 1965; McVittie, 1972*a*,*b*). We noted that the motility phenotypes of the suppressor and the *pf9-1* strains were strikingly similar. We therefore reexamined the original *pf9-1* strain and found that it, too, is an inner arm dynein mutant

Table I. Relationships between Different Inner Arm Mutations

Recombination tests	Segregation (PD:NPD:TT)	Conclusions
pf9-1 × *pf9-2*	60:0:0	<0.8 cM apart
pf9-2 × *ida1*	219:0:0	<0.2 cM apart
pf9-1 × *ida1*	98:0:0	<0.5 cM apart
pf9-2 × *ida4*	326:0:0	<0.15 cM apart
pf9-1 × *ida4*	98:0:0	<0.5 cM apart

Dominance tests

Genotype	Swimming phenotype	Conclusions
pf9-2 arg2 / + *arg7*	Wild-type	*pf9-2* is a recessive allele
pf9-1 arg7 / + *arg2*	Wild-type	*pf9-1* is a recessive allele
ida1 arg2 / + *arg7*	Wild-type	*ida1* is a recessive allele
ida4 arg7 / + *arg2*	Wild-type	*ida4* is a recessive allele

Complementation tests

Genotype	Swimming phenotype	Conclusions
pf9-2 arg2 / *pf9-1 arg7*	Mutant	Alleles at the same locus
pf9-2 arg7 / *ida1 arg2*	Mutant	Alleles at the same locus
pf9-1 arg7 / *ida1 arg2*	Mutant	Alleles at the same locus
pf9-2 + *arg2* / + *ida4 arg7*	Wild-type	Mutations at different loci
ida1 + *arg2* / + *ida4 arg7*	Wild-type	Mutations at different loci

(see below). On the basis of linkage, similarity of phenotype, and failure to complement *pf9-1*, we have designated the suppressor mutation *pf9-2*.

In the course of these experiments, we also observed that linkage groups XIII and XII are the same (Dutcher et al., 1991). Linkage group XII includes two closely linked inner arm dynein loci *IDA1* (*PF30*) and *IDA4* (Kamiya et al., 1991). Because of the similarity in the motility phenotypes of the *pf9* and *ida* mutations, we examined their relationship by recombination analysis (see Table I). The *pf9-1* and *pf9-2* alleles failed to recombine with either the *ida1* or the *ida4* mutation. These results indicate that these mutations are either alleles at the same locus or that these loci are simply closely linked. We distinguished between these two possibilities by pairwise complementation tests in stable diploid cell lines (Table I). Our data indicated that *pf9-1*, *pf9-2*, and *ida1* (*pf30*) are all recessive alleles at the same locus, and that this locus is distinct from that defined by the *ida4* mutation. This locus, which we know refer to as *PF9*, maps ~2 cM from *lf2* on the left arm of linkage group XII/XIII.

Interactions between the pf9-2 Mutation and Other Flagellar Mutations

Because the *pf9-2* mutation was obtained as a bypass suppressor of the *pf16BR3* mutant phenotype, we anticipated that *pf9-2* might exhibit a broad range of suppressor activity, similar to that described for other bypass suppressors (Huang et al., 1982*b*) and several other suppressors of *pf16* that we have identified (Dutcher, S. K., unpublished data). We therefore tested the *pf9-2* mutation in combination with other flagellar mutations (see Table II). We found that although *pf9-2* can suppress the flagellar paralysis associated with the *pf16BR3* allele at 32°C, it does not suppress the paralyzed flagellar phenotype associated with two nonconditional alleles of the *PF16* locus. Furthermore, recombinants of *pf9-2* with other central pair or radial spoke mutations have a more severely defective motility phenotype than either parent. Most double mutants are either aflagellate (when grown as vegetative cells) or assemble only short, immotile flagella (when grown as gametic cells). These data suggest that interaction between the *pf9-2* and *pf16BR3* mutations represents a specific interaction between the central pair microtubules and the inner dynein arms and not a more general bypass mechanism such as that shown by the *sup-pf-1* mutation (Huang et al., 1982*b*).

Because outer and inner arm dynein mutations differ in their motility phenotypes, we constructed recombinant dynein mutant strains to test if the motility defects would be

Table II. Interactions between pf9-2 and Other Flagellar Mutations

Mutant type and strain	Linkage group	Reference	Flagellar phenotype	Number of *pf9* recombinants examined	Double mutant phenotype
Central pair					
pf6	X	McVittie, 1972*a*; Dutcher et al., 1984	Slow twitch	30	Short, paralyzed flagella
pf16	IX	McVittie, 1972*a*; Dutcher et al., 1984	Fast twitch	35	Normal length, no suppression
pf16B (*ncs66*)	IX	Huang et al., 1979; Dutcher et al., 1984	Fast twitch	28	Normal length, no suppression
pf16BR3 (*ncs66R3*)	IX	Dutcher et al., 1984	Swim at 21°C Twitch at 32°C	37	Slow swimming at 21°C weak motility at 32°C
pf18	II	Adams et al., 1981	Paralyzed	2	Short, paralized flagella
pf19	X	Adams et al., 1981	Paralyzed	17	Short, paralyzed flagella
Radial spoke					
pf1	V	McVittie, 1972*a*	Paralyzed	10	Short, paralyzed flagella
pf27	XII/XIII	Huang et al., 1981	Paralyzed	66	Short, paralyzed flagella
Dynein arm					
pf3	VIII	McVittie, 1972*a*; Huang et al., 1982*b*	Slow swimming	15	Short, paralyzed flagella
pf13	IX	Huang et al., 1979	Paralyzed	3	Short, paralyzed flagella
pf22	I	Huang et al., 1979	Paralyzed	6	Short, paralyzed flagella
pf28	XI	Mitchell and Rosenbaum, 1985	Slow swimming	13	Short, paralyzed flagella
oda4	IX	Kamiya, 1988	Slow swimming	13	Short, paralyzed flagella
oda6	XII/XIII	Kamiya, 1988	Slow swimming	17	Short, paralyzed flagella
oda9	XII/XIII	Kamiya, 1988	Slow swimming	48	Short, paralyzed flagella
sup-pf-1 (*R6*)	IX	Huang et al., 1982*b*	Slow swimming	16	Normal length, slow wobble
Flagellar assembly					
fla5	XI	Adams et al., 1982	Wild-type at 21°C Aflagellate at 32°C	29	*pf9*-like motility at 21°C aflagellate at 32°C
fla10-1 (*dd-a-224*)	XIX	Huang et al., 1977	Wild-type at 21°C Aflagellate at 32°C	13	*pf9*-like motility at 21°C aflagellate at 32°C
lf2	XII/XIII	McVittie, 1972*a*,*b*	Long flagella	4	Short, paralyzed flagella or aflagellate
uni1	XIX	Huang et al., 1982*a*	Single flagellum	21	Aflagellate or slow uniflagellated
uni3	XIX	Huang et al., 1982*a*	Wild-type at 21°C Single flagellum at 32°C	14	*pf9*-like motility at 21°C at aflagellate or slow uniflagellated at 32°C

lf2, *pf28*, *oda4*, *oda6*, and *oda9* strains were obtained from the *Chlamydomonas* Genetics Center. All other strains were obtained from stocks maintained in this laboratory. Number of recombinants = (2 × NPD) + (TT).

synergistic (Table II). Double mutant strains that completely lack the outer arm and part of the inner arm (e.g., *oda4 pf9-2*, *oda6 pf9-2*, and *pf28 pf9-2*) are aflagellate or assemble only short, immotile flagella; the exact phenotype is again dependent on growth conditions. The immotile phenotype of these double mutants might be the direct result of the decrease in dynein arm activity or an indirect consequence of the reduced flagellar length. The former might reflect a requirement for a minimum number of active dynein arm subunits to achieve effective motility. The latter might simply reflect the loss of a proximally located structure required to either initiate or propagate flagellar movement. We have tried to distinguish between these possibilities by examining other double mutants and by analyzing revertants of the double mutant phenotypes (see below).

The dynein mutant *sup-pf-1* assembles morphologically normal outer arms, but the activity of the outer arm is altered, and the cells swim at approximately one-half their wild-type speed (Brokaw et al., 1982). The *pf9-2 sup-pf-1* recombinant strain assembles normal, full-length flagella, but the double mutant combines the wobbly swimming phenotype of *sup-pf-1* cells with the altered waveform of *pf9-2* cells (see Tables II and IV). These results indicate that inner and outer arm motility defects are synergistic and that the inner arm subunits that remain in *pf9-2* are sufficient to drive flagellar motility, but only if the flagella are of normal length.

The double mutant phenotypes described above indicate that defects in the dynein arms can have secondary effects on flagellar assembly. We therefore tested the *pf9-2* mutation in combination with a number of flagellar assembly mutations (see Table II). *Pf9* recombinants with mutant strains that assemble only a single flagellum (*unil*, *uni2*, and *uni3*) and mutant strains that assemble flagella of abnormal length (*lf2*) also have short, paralyzed flagella. Occasional, slow-moving, uniflagellate cells have been observed in the *uni pf9* double mutants, but these cells are usually <10% of the total population. These results indicate that the final extent of

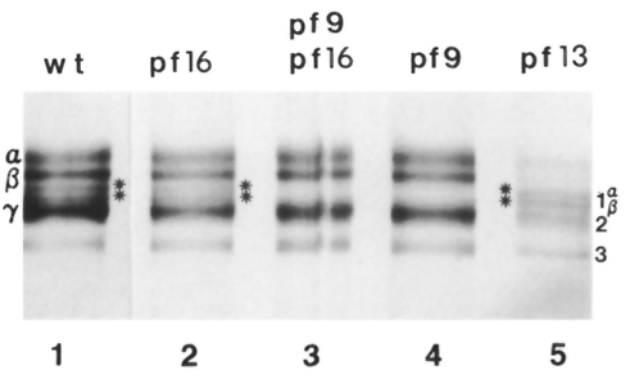

Figure 1. Dynein heavy chain composition of mutant strains. Axonemes were prepared from different mutant strains and analyzed by SDS-PAGE on a 3–5% polyacrylamide, 2–8 M urea gradient gel. Only the high molecular weight region (~400 kD) of the gel is shown here. From left to right, the samples are wild-type (*wt*), the central pair mutant *pf16BR3* (*pf16*), the original suppressed double mutant *pf16BR3 pf9-2* (*pf16pf9*), the *pf9-2* suppressor alone (*pf9*), and an outer dynein arm mutant *pf13* (*pf13*). Note the loss of bands 1α and 1β in *pf9* and the double mutant *pf16pf9*. Outer arm polypeptides are labeled α, β, and γ on the left. Inner arm polypeptides are labeled 1α, 1β, 2, and 3 on the right. Bands 2 and 3 contain two heavy chains each (Piperno et al., 1990), but appear as single broad bands on this gel. Stained with silver.

flagellar assembly in a particular strain is extremely sensitive to the presence or absence of the inner dynein arms.

The Motility Defect of the pf9-2 Mutation Cosegregates with a Deficiency of Four Axonemal Polypeptides

Axonemes isolated from *pf16BR3 pf9-2* cells grown at either 21 or 32°C are missing at least four axonemal polypeptides by SDS-PAGE analysis. An additional 10 polypeptides corresponding to the *pf16* signature polypeptides (Dutcher et al., 1984) are missing from *pf16BR3 pf9-2* axonemes isolated at 32°C. After recovery of the *pf9-2* mutation in a wild-type background, we found that the same four axonemal polypeptides are missing in axonemes obtained from either the double mutant or the *pf9-2* mutant alone. Two of the missing polypeptides correspond to inner arm dynein heavy chains (Fig. 1).

We examined the correlation between the *pf9* motility defect and the missing inner arm heavy chains by testing their ability to cosegregate in tetrad progeny and by comparing the biochemical phenotypes of both the *pf9-1* and *pf9-2* mutant alleles. The *pf9-2* flagellar phenotype cosegregated with the inner arm heavy chain defect in four independent tetrads (an example with two tetrads is shown in Fig. 2), and the *pf9-1* strain showed the same heavy chain defect.

We identified the dynein heavy chain species missing in *pf9* strains by comparison with other dynein mutants (see Fig. 3). The inner arm mutant *pf23* is deficient in five inner heavy chains, 1α, 1β, 2, 2′, and 3′ (Piperno et al., 1990; Piperno and Ramanis, 1991). Comparison of *pf9-2* and *pf23* axonemes (Fig. 3, lanes *1* and *5*) revealed that both lack polypeptides in the 1α/1β heavy chain region. The outer arm mutant *pf22* is deficient in outer arm heavy chains α, β, and γ and the inner arm heavy chains 2 and 3′, but it retains inner arm heavy chains 1α, 1β, 2′, and 3 (Piperno and Ramanis, 1991). Comparison of *pf22* with *pf9-2* demonstrated the presence of the 1α and 1β heavy chains in *pf22* axonemes (lane *6*) and their absence in *pf9-2* (lane *1*).

Defects in the phosphorylation of inner arm dynein heavy chains have also been reported in axonemes prepared from *pf2* and *pf3* strains, although the nature of these defects has not been well described (Luck and Piperno, 1989; Piperno et al., 1990). We examined the dynein heavy chain composition of these strains because of the similarity of their motility phenotypes (Brokaw and Kamiya, 1987) with that observed for *pf9*. Both the 1α/1β and the heavy chain region 3 polypeptides (containing heavy chains 2 and 3) are present in both *pf2* and *pf3* axonemes (Fig. 3, lanes *3* and *4*). The *pf9* heavy chain defect is therefore distinct from the defects observed in *pf2* and *pf3* axonemes.

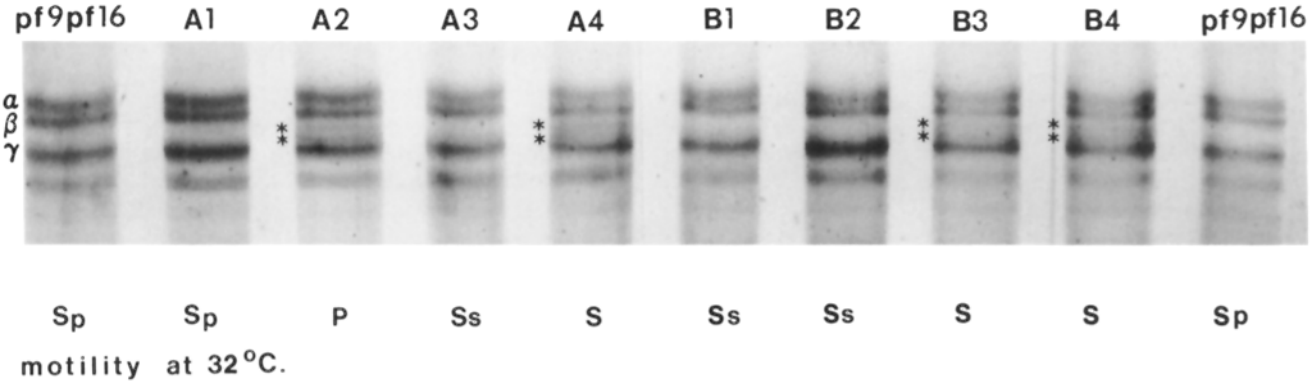

Figure 2. Cosegregation of the inner arm heavy chain defect with the *pf9* flagellar phenotype. Axonemes were prepared from the original *pf16BR3 pf9-2* strain and from strains grown up from the eight progeny of two tetrads and analyzed by SDS-PAGE on a 3–5% polyacrylamide, 2–8 M urea gel. The motility phenotypes of the cells at 32°C are indicated beneath each lane. The original *pf16pf9* strain was backcrossed to wild-type to yield the tetratype tetrad progeny A1–A4 (lanes *2–5*). The A1 strain contains both the *pf9* and the *pf16* mutations, and the *ts* flagellar paralysis is suppressed at 32°C. Liquid cultures of this strain contain more swimmers than pelleters, but the flagellar phenotype is abnormal (*Sp*). The A2 strain carries only the *pf16BR3* mutation, and it is paralyzed at high temperature (*P*). The A3 strain contains the new flagellar mutation, *pf9-2*, in a wild-type background. These cells swim slowly (*Ss*) at both the permissive and restrictive temperature for *pf16*. A4 is the wild-type progeny and swims normally (indicated as *S*) at 32°C. The A3 strain was crossed to wild-type to yield the tetrad progeny B1-B4. Note the 2:2 segregation of the inner arm heavy chain defect with the slow swimming phenotype.

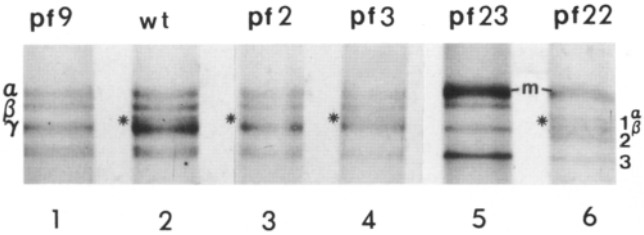

Figure 3. Dynein heavy chains in different inner arm dynein mutants. Axonemes were prepared from different flagellar mutants, and the dynein heavy chain region was compared by SDS-PAGE on a 3–5% polyacrylamide, 3–8 M urea gradient gel. Outer arm heavy chains are indicated on the left and inner arm heavy chains on the right. Contaminating flagellar membrane protein is indicated by the letter *m*. Approximately 1.5 μg of total axoneme protein was loaded in each lane, and the gel was silver stained. This gel does not resolve the inner arm heavy chain region 2 (containing inner arm heavy chains 2′ and 3′) and the outer arm γ chain well enough to draw conclusions about the relative abundance of these polypeptides, but the 1α/1β heavy chain region is indicated by asterisks.

Pf9 axonemes are also deficient for two intermediate chains of ~140 kD (137 ± 11, $n = 24$) and 110 kD (106 ± 10, $n = 21$). Because our observations differ from those reported previously (Goodenough et al., 1987; Piperno et al., 1990; Kamiya et al., 1991), we present four lines of evidence that demonstrate that these two intermediate chains are part of the same inner arm dynein subunit as the 1α and 1β heavy chains. First, the loss of these intermediate chains cosegregated with the *pf9-2* motility phenotype and the 1α/1β heavy chain defect in three tetrads. Second, we observed the same intermediate chain defect in high salt extracts of *pf9-1* axonemes. The gel shown in Fig. 4 *A* demonstrates the deficiency of the 140- and 110-kD polypeptides in high salt extracts of *pf9-1* (lane *1*) and *pf9-2* (lanes *2* and *3*) axonemes as compared with high salt extracts of both wild-type (lane *4*) and *pf28* (lane *5*) axonemes. Third, the missing 140- and 110-kD polypeptides are restored as a unit with the 1α and 1β heavy chains in intragenic revertants of the *pf9-2* mutant allele (see Figs. 4 *A* and 6).

Finally, the 140- and 110-kD polypeptides copurified with the 1α and 1β heavy chains as an 18S ATPase complex during chemical fractionation of wild-type and outer arm dynein mutant axonemes. Fig. 4 *B* shows the polypeptide profiles of the 18–19S region (Fractions 8 and 9) obtained from sucrose density gradients of four different dynein extracts. The wild-type sample (lanes *3* and *4*) contains a mixture of the outer arm 21S subunit and the inner arm 18S subunit. The outer arm polypeptides include the 69- and 78-kD intermediate chains as well as a 90-kD proteolytic fragment of the outer arm α heavy chain (King et al., 1986). The inner arm subunit contains a doublet of 140/138 kD and a 110-kD intermediate chain. The *pf9-2* sample (lanes *1* and *2*) contains the outer arm subunit polypeptides, but the polypeptides normally associated with the 18S inner arm subunit are missing. In contrast, the outer arm mutant *pf28* (lane *6*) is missing the 69- and 78-kD intermediate chains, but the polypeptides associated with the inner arm subunit are present. Both sets of polypeptides are missing in the double mutant *pf9-2 pf28* (lanes *7* and *8*). The results indicate that the polypeptide deficiency associated with the *pf9* mutation reflects the loss of a discrete inner arm subunit, the I1 subunit.

The independent behavior of the I1 subunit relative to the other inner arm subunits suggested to us that there might be experimental conditions under which the different inner arm subunits could be selectively extracted. We have found that the I1 subunit can be distinguished from the other inner arm subunits by its relative resistance to extraction by high concentrations of ATP. Incubation of *pf28* axonemes in 5–10 mM MgATP solubilizes ~40–50% of the axonemal ATPase activity (as measured by comparing *pf28* axonemes with ATP-extracted *pf28* axonemes). Sucrose density gradient centrifugation of the ATP extract resolves a broad peak of activity sedimenting at 12S, but little or no detectable ATPase activity in the 18S region (see Fig. 5). SDS-PAGE analysis of the gradient fractions indicates that the polypeptides of I1 inner arm subunit are detectable only at trace levels in the 18S region (Fig. 4 *B*, lane *5*). Reextraction of the ATP-treated axonemes in high salt–containing buffers releases an additional 40–50% of the axonemal ATPase (as measured by comparing *pf28* axonemes to high salt–extracted axonemes). Sedimentation of the high salt extracts resolves two peaks of ATPase activity at ~18S and 12S, respectively (Fig. 5). The 18S peak contains the polypeptides of the I1 subunit (Fig. 4 *B*, lane *6*). These results suggest that the I1 inner arm subunit is more tightly associated with the axoneme than other inner arm dynein subunits.

Isolation and Characterization of Revertants of the pf9-2 Mutation

The synergistic assembly defects observed with the various *pf9-2* double mutant strains (Table II) suggest that the inner dynein arms may play an important role in modulating flagellar assembly. Moreover, the short, paralyzed flagellar phenotypes of these double mutants provide a screen for new mutations in other loci that may control the assembly of the dynein arms and/or the flagella. We have used the *pf28 pf9* double mutant to isolate several classes of revertants by screening for motile cells after mutagenesis. Our initial screens have indicated that intragenic revertants are the largest group recovered, irrespective of the method of mutagenesis, but extragenic suppressors are found with reasonable frequency, especially with EMS treatment (see Table III).

The first class of mutants ($n = 22$) contains revertants of the *pf28* phenotype; these strains have full-length flagella and swim with a *pf9*-like motility phenotype. Analysis of isolated axonemes by SDS-PAGE demonstrates the recovery of the outer arm heavy chains α, β, and γ in all of these strains. Backcross data indicate that all of these revertants are the result of intragenic events at *pf28*. The second class contains revertants of the *pf9-2* phenotype ($n = 33$); backcross data indicate that 31 of these strains are intragenic revertants of *pf9-2* and 2 (*R13* and *E5*) are extragenic suppressors. Typical examples of the *pf9-2* revertants are described next.

R11 is an intragenic revertant of the *pf9-2* allele. The *pf28 pf9-2R11* strain assembles full-length flagella and is indistinguishable from *pf28* in its motility phenotype (see Table IV). We isolated the *pf9-2R11* allele in a wild-type background by backcrossing *pf28 pf9-2R11* to a *pf9-2* strain. The motility phenotype of the *pf9-2R11* allele is indistinguishable from wild-type. The 1α/1β heavy chains (Fig. 6, compare lanes *5–7*) and the 140- and 110-kD intermediate chains are also restored in both the original *pf28 pf9-2R11* strain (Fig. 4 *A*,

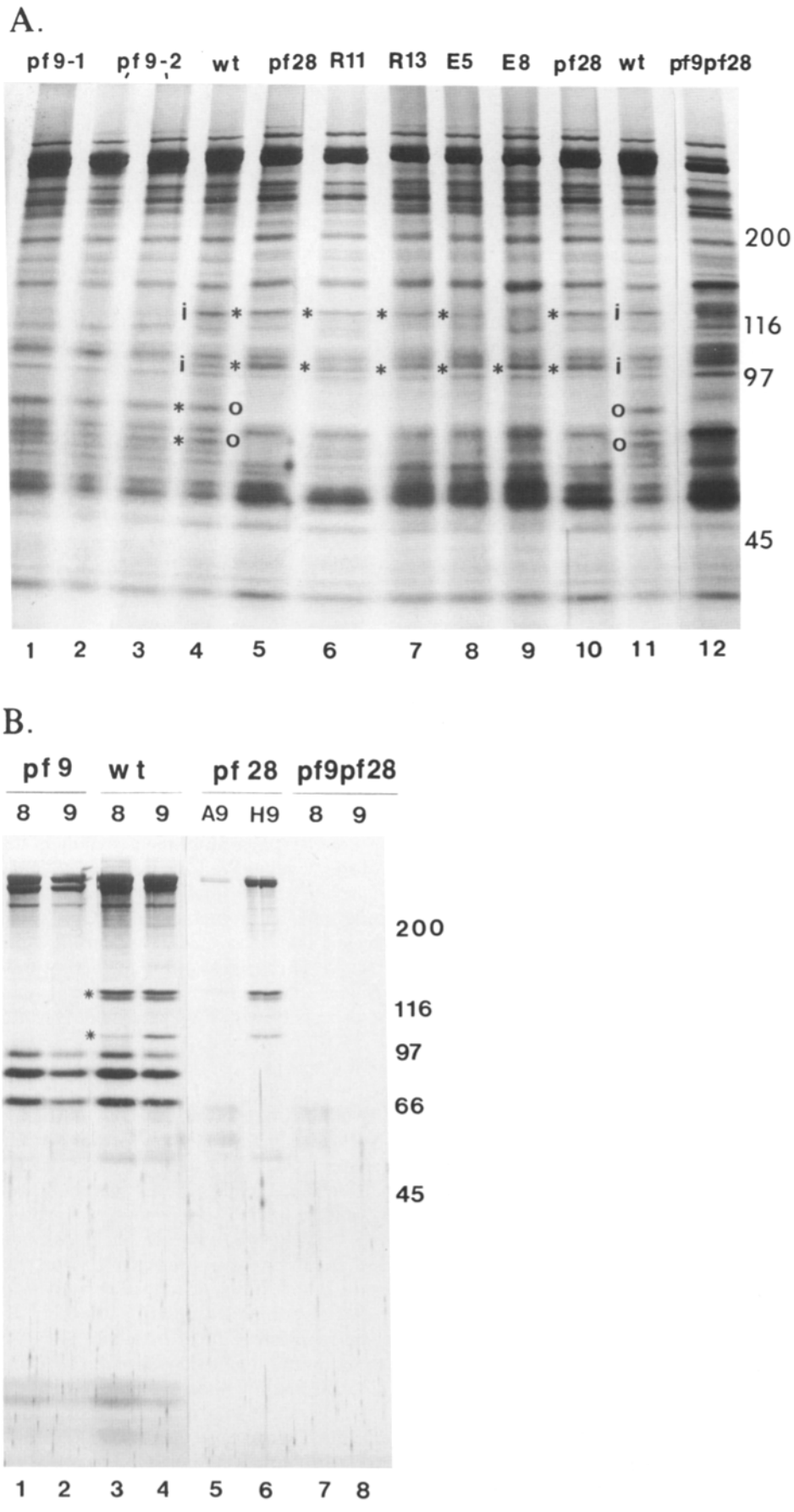

Figure 4. Intermediate chain composition of different dynein mutants. (*A*) High salt extracts of axonemes were prepared from different mutant strains and analyzed by SDS-PAGE on a 5–15% polyacrylamide gradient gel. 1.5 μg protein was loaded per lane, and the gel was silver stained. The positions of the molecular weight standards are indicated on the right. Outer arm intermediate chains (*o*) and a subset of the inner arm intermediate chains (*i*) are indicated adjacent to the lanes of the wild-type samples. Strains that contain the 140- and 110-kD polypeptides are indicated with asterisks. (*B*) Dyneins were purified from different mutant strains by ATP or high salt extraction and sucrose density gradient centrifugation. The polypeptide composition of the 18–19S region from parallel gradients was compared by SDS-PAGE on a 5–15% polyacrylamide gradient gel. From left to right: Lanes *1* and *2*, fractions 8 and 9 from a high salt extract of *pf9-2* axonemes. Lanes *3* and *4*, fractions 8 and 9 from a high salt extract of wild-type axonemes. Lane *5*, fraction 9 from an ATP extract of *pf28* axonemes. Lane *6*, fraction 9 from a high salt extract of *pf28* axonemes. Lanes *7* and *8*, fractions 8 and 9 from a high salt extract of *pf9-2 pf28* axonemes. No ATPase activity or dynein polypeptides were detected in the 19S region of the *pf28 pf9-2* gradient. The positions of the molecular weight standards are indicated on the left. The intermediate chains that cosediment with the I1 inner arm subunit are indicated by asterisks. The 140/138-kD doublet deserves further comment. We have observed the 138-kD polypeptide in all our 18S dynein samples prepared from both wild-type and *pf28* axonemes. This polypeptide stains differentially with silver, and it may represent an isoelectric variant as described by Goodenough et al. (1987) or it may simply be a proteolytic fragment.

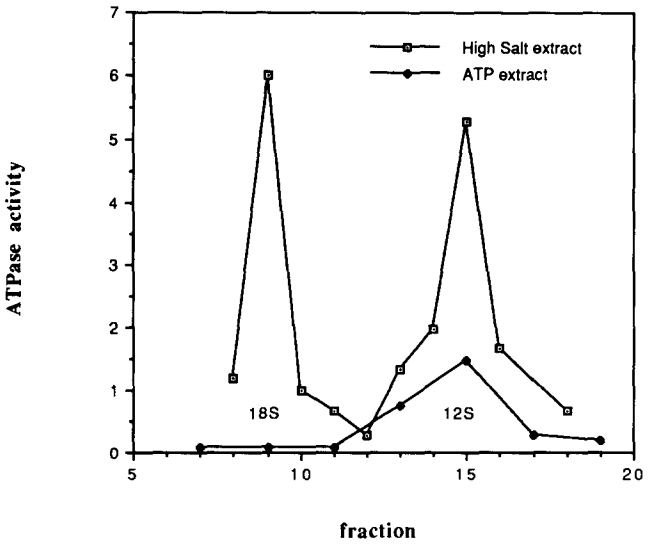

Figure 5. Differential extraction of inner arm dynein ATPases. *pf28* axonemes were extracted sequentially in 10 mM MgATP (ATP extract) and the 0.6 M KCl (high salt extract). The total ATPase activity present in the whole axonemes, the ATP-treated anonemes, and the high salt extracted axonemes was then determined. The ATP and high salt extracts were dialyzed against buffer and then fractionated by sucrose density gradient centrifugation. The relative ATPase activities present in the gradients of the ATP extract (*closed squares*) and high salt extracts (*open squares*) are shown here. The total ATPase activity recovered from the gradients is greater in the high salt extract than in the ATP extract, in part because the high salt treatment activates the dynein ATPase.

lane *6*) and the *pf9-2RI1* strain. Sucrose density gradient centrifugation of high salt extracts demonstrates full recovery of the 18S ATPase activity and the four polypeptides missing in *pf9* (Table IV and data not shown). These results are consistent with the hypothesis that these four polypeptides form the I1 inner arm subunit.

R13 is an unlinked, interactive suppressor of the *pf9-2* allele; the triple mutant *pf28 pf9-2RI3* has a motility phenotype similar to that of *pf28* (see Table IV), although a given population of cells can be more erratic in its swimming behavior than *pf28* cells. SDS-PAGE analysis of axonemes prepared from the triple mutant demonstrates the partial recovery of the 1α and 1β heavy chains (Fig. 6, lane *I*) and 140- and 110-kD polypeptides (Fig. 4 *A*, lane *7*). Sucrose density gradient centrifugation indicates that both 18S ATPase activity and I1 subunit polypeptides are restored (Table IV and data not shown). However, the extent of the recovery of both the ATPase activity and all four polypeptides varies between preparations. These results suggest that the I1 inner arm subunit may be altered and/or less stable in the R13 strains. Similar results have been observed with the extragenic suppressor E5.

Table III. Reversion Analysis of pf28 pf9-2

Mutagen	Total revertants	Intragenic		Extragenic
		pf28	*pf9-2*	
Irradiation				
Ultraviolet	17	6	10	1
Gamma ray	21	11	10	0
Chemical				
DEB	6	0	6	0
EMS	12	5	5	2
Total	56	22	31	3

Our procedures for mutagenesis and screening of the *pf28 pf9-2* double mutant are described in Materials and Methods. Each isolate was backcrossed to wild-type, and each revertant was identified as intragenic or extragenic based on an average of 18 tetrads apiece.

The third extragenic revertant (E8) is a bypass suppressor of the *pf9-2 pf28* interaction with an unusual motility phenotype. The E8 strain does not rescue either the *pf28* or the *pf9* phenotype, but the triple mutant does assemble two full-length or longer flagella (see Table IV). The majority of these cells are, however, barely motile. Some cells are completely paralyzed, others twitch the tips of their two flagella occasionally, and still others swim in slow circles with one flagellum paralyzed while the second one beats. Measurements of axonemal ATPase activity and sucrose density gradient analysis of E8 dynein extracts indicate that both the outer arm dynein subunits and the 18S inner arm dynein subunit are still missing (data not shown), although a 110-kD polypeptide has been observed in high salt extracts of E8 axonemes (Fig. 4 *A*, lane *9*). These data demonstrate that the flagellar assembly defects observed with the different *pf9-2* double mutants described in Table II do not reflect a specific requirement for the entire I1 subunit in order to achieve wild-type flagellar length. However, the recovery of full-length flagella in the E8 revertant is not sufficient to restore flagellar motility. These results indicate that it is possible to use the *pf9-2 pf28* double mutant to identify loci that affect flagellar assembly independently of flagellar motility.

Structural Phenotypes of Inner Arm Mutations

Because our biochemical data indicated that the *pf9* mutations resulted in the loss of a discrete inner arm subunit, we examined the structural phenotypes of these strains by thin-section electron microscopy. As will be shown below and in the accompanying paper by Mastronarde et al. (1992), our results indicate that the polypeptides missing in *pf9* form a distinct domain within the row of the inner dynein arms.

We compared the images of cross-sections of wild-type and mutant axonemes. Initial results indicated that the images of the inner dynein arms were weaker in *pf9* axonemes than in wild-type axonemes, but the precise morphological defect was unclear (McDonald, K. L., and M. E. Porter, data not shown). We reasoned that if the polypeptides missing in *pf9* form only one of several inner arm subunits, then the average of a large number of cross-sections cut at randomly chosen positions along the length of the axoneme should give a more reliable image of the mutant defect.

Fig. 7, *A* and *B*, show typical averages of wild-type and *pf9-2* samples, with contour lines drawn at levels of constant staining density. The appearance of the *pf9-2* sample differs from the wild-type sample most dramatically in the shape of the contour lines around the outer domain of the inner arm, but staining is decreased over the entire arm (note that the top contour line in *pf9* is lower than the top contour line in wild-type). These differences have been confirmed in all mutant alleles of the *pf9* examined thus far (see Fig. 4 of Mastronarde et al., 1992). We infer that the polypeptides as-

Table IV. Motility and ATPase Activity of Dynein Mutants

Strain	Motility phenotype	Swimming velocity	Flagellar length	Axonemal ATPase activity	18S ATPase activity
		μm/s (n)	*μm (n)*	*nmol/(min × mg)*	*% of total*
Wild-type	Normal	152 ± 23 (25)	10.4 ± 1.2 (44)	297	
pf9-2	Slow swimming	54 ± 12 (26)	11.4 ± 1.5 (57)	297	
pf28	Wobble	38 ± 6 (26)	11.9 ± 1.7 (53)	59	22
pf28 pf9-2	Paralyzed		4.4 ± 0.8 (55)	37	
pf28 pf9-2 R11	Wobble	42 ± 9 (25)	11.0 ± 1.6 (64)	49	23
pf28 pf9-2 R13	Wobble	35 ± 8 (26)	12.1 ± 1.6 (47)	46	22
pf28 pf9-2 E5	Wobble	39 ± 9 (16)	11.2 ± 1.8 (50)	59	18
pf28 pf9-2 E8	Paralyzed		13.8 ± 2.2 (56)	27	6
sup-pf-1	Wobble	72 ± 10 (25)			
sup-pf-1 pf9-2	Slow wobble	50 ± 7 (25)			

Swimming velocities and flagellar lengths are expressed as mean ± standard deviation (n = sample size). Axonemal ATPase activities are the averages obtained from two or more independent preparations of whole axonemes. 18S ATPase activity is expressed as the percentage of the total ATPase activity recovered on a sucrose density gradient of a high salt extract.

sociated with the I1 inner arm subunit span both the inner and outer domains of the inner dynein arm.

A similar difference is observed between the inner arms of the *pf28* and *pf28 pf9-2* samples (Fig. 7, *C* and *D*). The absence of the outer arm in *pf28* strains does not appear to alter the staining characteristics of the inner arm (compare *7c*, *pf28*, and *7a*, *wild-type*), and furthermore, the cross-sectional profile of the inner arm in the short, double mutant *pf9-2 pf28* (Fig. 7 *D*) is very similar to its profile in *pf9-2* alone (Fig. 7 *B*). These results indicate that the appearance of the inner dynein arm is not noticeably altered by changes in flagellar length, in spite of possible changes in inner arm polypeptide composition (Piperno and Ramanis, 1991).

We also examined the structure of the inner arm in the intragenic and extragenic revertants of the *PF9* locus. The recovery of inner arm polypeptides in the intragenic revertant *pf28 pf9-2R11* is associated with the restoration of inner arm density to an essentially wild-type appearance (Fig. 7 *E*). Some small differences in the contour lines are visible, but these are not statistically significant (see Mastronarde et al., 1992). These results are consistent with our observations that both the motility and biochemical phenotypes of the *pf9-2R11* allele are essentially wild-type.

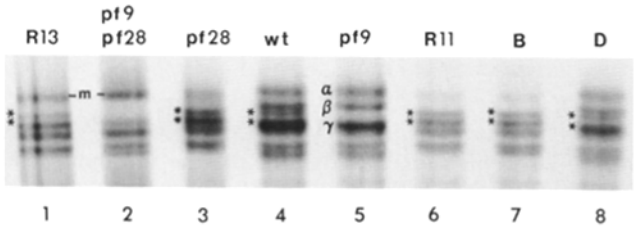

Figure 6. The recovery of the 1α and 1β heavy chains in extragenic and intragenic revertants of *pf9-2*. The intragenic revertant *pf28 p9-2R11* was crossed to a *pf9-2* strain to obtain the revertant allele in a wild-type background. Axonemes were then prepared from different mutant and revertant strains and analyzed by SDS-PAGE on a 3–5% polyacrylamide, 2–8 M urea gradient gel. From left to right: (*1*) the triple mutant *pf28 pf9-2 R13*, (*2*) the *pf28 pf9-2* double mutant, (*3*) the outer arm mutant *pf28*, (*4*) wild-type, (*5*) the *pf9-2* strain, (*6*) the original *pf28 pf9-2R11* revertant, (*7*) progeny B (a nonrecombinant *pf28 pf9-2R11* strain), and (*8*) progeny D (the *pf9-2R11* allele in a wild-type background). Note the recovery of the 1α and 1β heavy chains (indicated by asterisks) in the *R11* strains. (Band 1β is not well resolved from the γ heavy chain of the outer arm dynein in this gel. The large band marked *m* in lanes *1* and *2* is contaminating membrane protein.)

The extragenic revertant *R13*, however, presents a much more complex phenotype. The panel shown in Fig. 7 *F* is the grand average of five independently prepared samples representing 418 outer doublets from the *pf28 pf9-2R13* strain. The image of the inner arm in this final average is intermediate in phenotype between that of *pf28 pf9-2* and *pf28*. Density has been restored, as indicated by the height of the contour lines, but the shape of the inner arm in the outer domain is not wild-type. Reexamination of the different R13 preparations indicates that the apparent structure of the inner arm in the *R13* strain varies between different samples. Some samples appear similar to *pf28*, whereas others are closer to *pf28 pf9-2*. This result is not surprising in the context of the variable flagellar and biochemical phenotype associated with this triple mutant strain. However, the problem of intersample variability in this strain demonstrated to us the need for more quantitative methods with which to compare these mutant strains. The results from such developments are shown in the accompanying paper (Mastronarde et al., 1992).

Discussion

Extragenic Suppressors and Dynein Arm Mutations

Mutations in *Chlamydomonas* that disrupt the radial spoke and central pair structures generally lead to flagellar paralysis, and current models of flagellar movement suggest that this paralysis is the result of global inactivation of dynein arm activity (Huang et al., 1982*b*). The discovery of second site suppressors that restore flagellar movement without altering the original central pair or radial spoke assembly defects indicated the presence of a second control system in the axoneme (Huang et al., 1982*b*). This control system is proposed to inhibit the activity of the dynein arms in the absence of a signal from the radial spoke–central pair complex. This inhibition leads to paralysis in radial spoke and central pair defective strains. The second site or extragenic suppressors are thought to short circuit this control system and allow

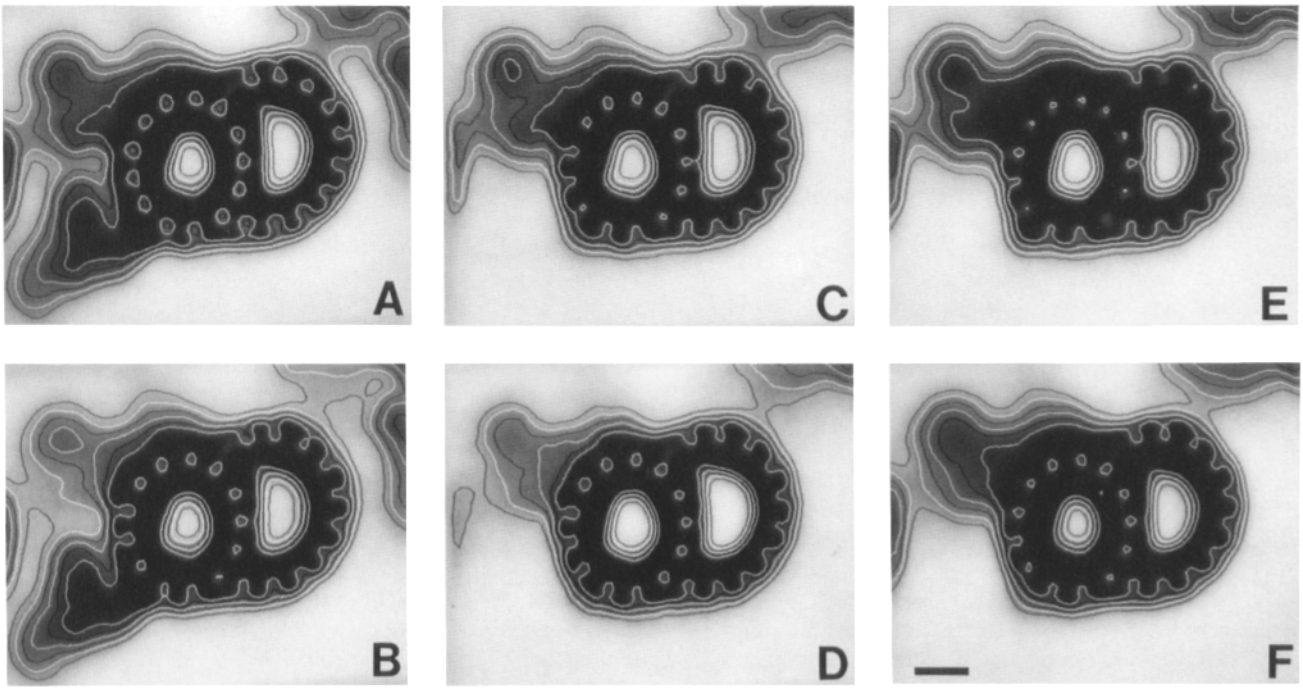

Figure 7. Structural phenotypes. Axonemes were prepared from different mutant strains and examined in cross-section by standard transmission electron microscopy. Images of the dynein arms are shown here after computer averaging of multiple outer doublets. The inner arm is displayed on the top and the outer arm on the bottom. The total number of doublets used to compute each average is indicated (*n*). (*A*) Wild-type (n = 337). (*B*) *pf9-2* (n = 235). (*C*) *pf28* (n = 225). (*D*) *pf9-2 pf28* (n = 148). (*E*) *pf28 pf9-2R11* (n = 237). (*F*) *pf28 pf9-2R13* (n = 418). This figure was prepared from images obtained by Kent McDonald and processed by Eilleen O'Toole and David Mastronarde. For details of methods, see Mastronarde et al. (1992). Bar, 10 nm.

dynein arm activity in the absence of a normal signal from the radial spoke–central pair complex. The nature of this control system has been only poorly understood.

By analyzing mutations obtained in a screen for suppressors of flagellar paralysis, we have identified a new inner dynein arm mutation, *pf9-2*. The *pf9-2* mutation differs from all of the suppressors previously described both in its range of suppression and in its biochemical and structural phenotype. In particular, *pf9-2* is the first extragenic suppressor that identifies the I1 inner arm subunit as a potential site for the regulation of flagellar motility. Preliminary studies with other suppressors of *pf* mutant strains in our collection indicate that they also identify new loci with novel phenotypes (Dutcher et al., 1988, this report, and M. Porter and S. K. Dutcher, unpublished observations). We have found that some of these suppressors may also act by altering the structures associated with the inner dynein arms (Mastronarde et al., 1992; S. King, W. B. Inwood, J. Power, E. O'Toole, and S. K. Dutcher, manuscript in preparation). These observations provide the first evidence on the likely location of the radial spoke and central pair control system.

The frequency with which inner arm mutations appear at the *PF9* locus is striking. The original mutant allele, *pf9-1*, was first described nearly thirty years ago as an abnormal swimming mutation (Hastings et al., 1965; McVittie, 1972*a*,*b*), but no description of its biochemical or structural phenotype was available. We have shown that *pf9-1* and *pf9-2* are alleles at the same locus by both complementation and recombination tests, and we have since confirmed their common biochemical and structural phenotypes (see Fig. 4 and Mastronarde et al., 1992). We have also shown that the *ida1* allele fails to complement both the *pf9-1* and *pf9-2* alleles, but that complementation is observed between *ida4* and *pf9-2* alleles (Table II). These results indicate that the *PF9* locus is represented by at least nine different mutant alleles known variously as *pf9* (two strains), *ida1* (six strains), and *pf30* (one strain).

It seems likely that the *PF9* locus might be the structural gene for one of the I1 subunit polypeptides, but as yet the *PF9* gene product has not been identified. We have isolated 31 intragenic revertants of the *pf9-2* allele (Table III), but all these revertants are completely wild-type with respect to their swimming phenotype, and no conditional allele has yet been identified. We have attempted to identify the *PF9* gene product by dikaryon rescue analysis, but our initial experiments have been inconclusive. These observations suggest that productive study on the identity of the *PF9* gene product must await either the application of new screens for conditional revertants and/or the development of molecular probes for inner arm polypeptides.

Interactions between pf9-2 and Other Flagellar Mutations

One of the more interesting aspects of the *pf9-2* mutation is the complexity of its interactions with other mutations that affect both flagellar motility and assembly. The suppression by *pf9* of mutations at the *pf16* locus is allele specific at both loci. These observations imply that the restoration of flagellar motility in the suppressed strain depends on a particular alteration in the *PF9* gene product that compensates for the defect in the central pair microtubules in *pf16BR3*. Although

the mechanism of suppression is not well understood for any flagellar mutation, we have observed similar allele specificity with other suppressor loci (Lux and Dutcher, 1991, and M. E. Porter and S. K. Dutcher, unpublished data). A better understanding of the mechanism of suppression may depend on the identification of the *PF9* gene product.

In most cases, the loss of the I1 inner arm subunit in *pf9-2* is synergistic with the assembly defects of other flagellar mutations irrespective of the specific structure that is affected. Most of the double mutant strains assemble short, immotile flagella (see Table II). Synergistic flagellar assembly defects have also been observed with other inner arm mutations and other flagellar mutations (Kamiya et al., 1989, 1991; Mitchell and Yang, 1991; Piperno and Ramanis, 1991). These results suggest that axoneme length in a given strain may reflect a requirement for some minimum number of stable parts, not a specific requirement for a particular allele or a particular structure, such as the I1 inner arm subunit.

The short, immotile phenotype of some double mutant strains has, however, proven extremely useful for the identification of new mutations. We have used the *pf28 pf9-2* double mutant to isolate two new classes of extragenic suppressors: interactive suppressors that restore missing inner arm polypeptides (R13 and E5) and a bypass suppressor that restores wild-type flagellar length (E8). The R13 and E5 mutations are the first interactive suppressors of a dynein arm mutation to be identified. It seems likely that these suppressors may identify the loci of structural genes for inner arm polypeptides. Future study of this class will be useful in identifying the different loci that regulate assembly of the inner dynein arm subunits.

Flagellar Length and Flagellar Motility

Virtually all of the double mutant strains that we have examined are paralyzed. Since many of the combinations involve strains with impaired motility, it is not too surprising that they become paralyzed. However, double mutant strains constructed from motile, but slowly swimming parents (e.g., *oda4 pf9*, *pf28 pf9*) also have short flagella and are paralyzed. The immotile phenotype of the double dynein mutants may reflect a requirement for a minimum number of active dynein arm subunits to achieve effective motility. However, it is difficult to discern whether flagellar paralysis in these strains is the direct result of the decrease in dynein arm activity or a secondary consequence of the reduced flagellar length. In a recent study, Piperno and Ramanis (1991) have demonstrated that mutants with flagella <6 μm long are deficient for inner arm heavy chains 2 and 3′. They propose that the deficiency in the 3′ heavy chain subunit may be directly responsible for the flagellar paralysis observed in short flagellar mutants.

The best argument for a role of flagellar length in motility is the difference in the behavior of the *oda4 pf9-2* double mutant strain from the *sup-pf-1 pf9-2* double mutant strain. *Sup-pf-1* and *oda4* are two mutations at the *SUP-PF-1* locus, a locus that is thought to encode the β heavy chain of the outer arm dynein (Huang et al., 1982*b*; Kamiya, 1988; Porter, M. E., Power, J., and S. K. Dutcher, manuscript in preparation). Both mutants swim with a reduced flagellar beat frequency (Brokaw and Kamiya, 1987). However, the *sup-pf-1* strain assembles the outer dynein arm (Huang et al., 1982*b*), whereas the *oda4* strain does not (Kamiya, 1988). *oda4 pf9-2* strains have short, paralyzed flagella, but *sup-pf-1 pf9-2* strains assemble flagella of wild-type length and swim with a slow, wobbly motility phenotype. These results indicate that a simple reduction in inner and outer dynein arm activity does not by itself lead to flagellar paralysis and further suggest that the change in flagellar length in *oda4 pf9-2* is responsible for the paralysis phenotype. Given the heterogeneity of structures that occur along the length of the flagellum (Hoops and Witman, 1983; Piperno and Ramanis, 1991), it is possible that the absence of a specific structure in short flagella could render the remaining dynein arm subunits insufficient to achieve motility.

It is clear, however, that changes in flagellar length are neither necessary nor sufficient to restore flagellar motility. First, as shown by Piperno and Ramanis (1991), extragenic suppressors such as *sup-pf-3* can restore some degree of flagellar motility to short flagellar mutants without changes in flagellar length or the composition of dynein heavy chains. Second, the recovery of full-length flagella in the extragenic revertant E8 is insufficient to restore motility to the paralyzed *pf28 pf9-2* strain, even though the in vitro sliding velocity of axonemes from the triple mutant is equal to that observed for *pf28* axonemes (Sale, W. S., and E. F. Smith, personal communication). This bypass suppressor assembles full-length flagella without restoring the missing inner arm or outer arm subunits. The further study of the E8 revertant may provide evidence on the identity of the components that are altered in short, paralyzed flagella. It will be of interest to determine if any of the other inner arm polypeptides are altered in the E8 revertant strain.

Polypeptide Composition of the I1 Inner Arm Subunit

We have presented several lines of evidence indicating that the four polypeptides missing in *pf9* strains form the I1 inner arm subunit. These include the cofractionation of these polypeptides with the 18S ATPase activity in wild-type and *pf28* samples, the loss of these polypeptides in *pf9* strains, and the recovery of these polypeptides in intragenic revertants of *pf9-2*. These observations are consistent with the polypeptide phenotype reported for another *PF9* allele, *pf30* (Luck and Piperno, 1989), but different from that described for the *ida1* allele (Kamiya et al., 1991).

Our results also differ from some earlier reports concerning the cofractionation of the 110-kD polypeptide with the 18S inner arm subunit in *pf28* extracts. Previous investigators have identified a 140-kD polypeptide as a component of the 18S–21S inner arm complex (Goodenough et al., 1987; Piperno et al., 1990), but under their experimental conditions the 110-kD polypeptide was always found in the 12.7S region of the gradient (Goodenough et al., 1987). These studies differ from ours in the use of higher salt concentrations during sucrose density gradient centrifugation, which could lead to subunit dissociation. More recently, Smith and Sale have reported the purification of the I1 subunit using buffer conditions similar to ours, and they have observed the cofractionation of both a 140-kD and a 97-kD component with the 1α/1β heavy chains (Smith and Sale, 1991). We think it likely that their 97-kD component is equivalent to our 110-kD polypeptide, and that the discrepancy in molecular weights is due primarily to differences in electrophoretic conditions.

Previous studies had indicated that a subfraction of the

outer dynein arms could be solubilized by exposure to high concentrations of ATP (Goodenough and Heuser, 1984). We have used a similar approach in an effort to identify conditions for the selective solubilization of inner arm components. Our results indicate that the ~40–50% of I2 and I3 inner arm subspecies can be selectively solubilized by ATP treatment, and that the I1 subunit is more resistant to ATP extraction. These results are consistent with the idea that the different inner arm subunits have different affinities for their microtubule binding sites in the axoneme. These observations may also be useful in establishing conditions for the fractionation of the multiple I2 and I3 subspecies.

Location of the I1 Inner Arm Subunit

Our preliminary structural analysis of the *pf9* mutant and revertant strains indicates that the polypeptides of the I1 inner arm subunit occupy a distinct inner arm location. Computer-aided image analysis of wild-type and mutant strains reveals the loss of inner arm density in *pf9* axonemes, the recovery of inner arm density in the R11 intragenic revertant, and the variable recovery of inner arm density in the R13 extragenic revertant (Fig. 7). Qualitative inspection of these averages suggests that although most of the density lost in *pf9* axonemes is located in the domain adjacent to the outer arms, some density is also lost in the domain adjacent to the central pair and radial spokes. These results are inconsistent with a model in which the I1 subunit is present in only one of two inner arm rows (Kamiya et al., 1991). An alternative model is that the I1 subunit is attached to the wall of the outer doublet microtubule at an angle that is slightly skewed from the remaining inner arm subunits. We have examined this hypothesis and present our current model of inner arm structure in the accompanying paper (Mastronarde et al., 1992).

Functions of the Inner Dynein Arms in Flagellar Motility

Several lines of evidence suggest that the inner and outer dynein arms have different functions in the generation of flagellar motility. Most mutant strains that lack the outer arms swim with a normal flagellar waveform, but with a reduced flagellar beat frequency (Mitchell and Rosenbaum, 1985; Kamiya, 1988). These observations suggest that the inner dynein arms are sufficient for normal motility, and that the primary function of the outer dynein arms is to provide additional power for force generation. Mutants that lack a subset of inner dynein arm subunits swim with altered flagellar waveforms, but at near wild-type beat frequencies (Brokaw and Kamiya, 1987; Kamiya et al., 1991). Mutants that lack two or more inner arm subunits are paralyzed (e.g., *ida2/ida4*), but can undergo sliding disintegration in vitro at near wild-type velocities (Kurimoto and Kamiya, 1991). These results indicate that although the rates of both sliding velocity and beat frequency are dominated by the outer dynein arms, the inner dynein arms provide an essential function required to generate the flagellar waveform. One of these functions is likely to be the response to signals from regulatory elements such as the radial spokes and/or central pair. Our observations with the *pf9* mutations are consistent with this model. Loss of the I1 subunit in *pf9-2* has only minor effects on the flagellar beat frequency and axonemal ATPase activity (Table IV), but can suppress the flagellar paralysis in *pf16BR3* strains. Although the mechanism of suppression is not well understood, these observations provide the first evidence linking the functions of the inner dynein arms and the central pair microtubules in controlling flagellar motility.

The *pf16BR3* suppressors were isolated with the help of Zenta Ramanis while one of us (S. K. Dutcher) was a National Institutes of Health postdoctoral fellow in the laboratory of David Luck. M. E. Porter would like to acknowledge David Luck for encouragement to pursue the analysis of these suppressors. The *ida1* and *ida4* strains were generously provided by Dr. R. Kamiya. M. E. Porter would also like to acknowledge Jodi Goldberg for expert technical assistance, and Richard McIntosh and David Mastronarde for helpful comments on the manuscript.

This work was supported by National Science Foundation grants to S. K. Dutcher and M. E. Porter (DCB8518224 and DCB9005079) and an NIH grant (RR-00592) to the Laboratory for 3-Dimensional Fine Structure, J. R. McIntosh, director. Additional support to M. E. Porter was provided by start-up funds from the Graduate School of the University of Minnesota, the Minnesota Medical Foundation, the University of Minnesota's American Cancer Society Institutional grant IN-30-28, and the Mcknight-Land Grant Professorship. This work was also aided in part by a Basil O'Connor Starter Scholar Research Award (5-FY91-0607) from the March of Dimes Birth Defects Foundation.

Received for publication 21 February 1992 and in revised form 19 May 1992.

References

Adams, G. M. W., B. Huang, G. Piperno, and D. J. L. Luck. 1981. The central pair microtubular complex of *Chlamydomonas* flagella. Polypeptide composition as revealed by analysis of mutants. *J. Cell Biol.* 91:69–76.

Adams, G. M. W., B. Huang, and D. J. L. Luck. 1982. Temperature sensitive assembly-defective flagella mutants of *Chlamydomonas reinhardtii*. *Genetics.* 100:579–586.

Bradford, M. 1976. A rapid and sensitive method for quantitation of microgram quantities of proteins utilizing the principle of protein-dye binding. *Anal. Biochem.* 72:248–284.

Brokaw, C. J., and R. Kamiya. 1987. Bending patterns of *Chlamydomonas* flagella: IV. Mutants with defects in inner and outer dynein arms indicate differences in dynein arm function. *Cell Motil. Cytoskeleton.* 8:68–75.

Brokaw, C. J., D. J. L. Luck, and B. Huang. 1982. Analysis of the movement of *Chlamydomonas* flagella. The function of the radial spoke system is revealed by comparison of wild type and mutant flagella. *J. Cell Biol.* 92:722–732.

Dutcher, S. K., B. Huang, and D. J. L. Luck. 1984. Genetic dissection of the central pair microtubules of the flagella of *Chlamydomonas reinhardtii*. *J. Cell Biol.* 98:229–236.

Dutcher, S. K., W. Gibbons, and W. B. Inwood. 1988. A genetic analysis of suppressors of the *PF10* mutation in *Chlamydomonas reinhardtii*. *Genetics.* 120:965–976.

Dutcher, S. K., J. Power, R. E. Galloway, and M. E. Porter. 1991. Reappraisal of the genetic map of *Chlamydomonas reinhardtii*. *J. Hered.* 82:295–301.

Ebersold, W. T. 1967. *Chlamydomonas reinhardi*: heterozygous diploid strains. *Science (Wash. DC).* 157:446–449.

Eversole, R. A. 1956. Biochemical mutants of *Chlamydomonas reinhardi*. *Am. J. Bot.* 43:404–407.

Gibbons, I. R. 1988. Dynein ATPases as microtubule motors. *J. Biol. Chem.* 263:15837–15840.

Goodenough, U. W., and J. E. Heuser. 1984. Structural comparison of purified dynein proteins with *in situ* dynein arms. *J. Mol. Biol.* 180:1083–1118.

Goodenough, U. W., and J. E. Heuser. 1989. Structure of the soluble and *in situ* ciliary dyneins visualized by quick-freeze deep-etch microscopy. *In* Cell Movement. Vol. 1. F. D. Warner, P. Satir, and I. R. Gibbons, editors. Alan R. Liss, Inc., New York. 121–140.

Goodenough, U. W., B. Gebhart, V. Mermall, D. R. Mitchell, and J. E. Heuser. 1987. High pressure liquid chromatography fractionation of *Chlamydomonas* dynein extracts and characterization of inner-arm dynein subunits. *J. Mol. Biol.* 194:481–494.

Harris, E. H. 1989. The *Chlamydomonas* Sourcebook. Academic Press, San Diego. 780 pp.

Hastings, P. J., E. E. Levine, E. Cosbey, M. O. Hudock, N. W. Gillham, S. J. Surzycki, R. Loppes, and R. P. Levine. 1965. The Linkage groups of *Chlamydomonas reinhardi*. *Microb. Genet. Bull.* 23:17–19.

Holmes, J. A., and S. K. Dutcher. 1989. Cellular asymmetry in *Chlamydo-*

monas reinhardtii. J. Cell Sci. 94:273–285.
Hoops, H. J., and G. B. Witman. 1983. Outer doublet heterogeneity reveals structural polarity related to beat direction in *Chlamydomonas flagella. J. Cell Biol.* 97:902–908.
Huang, B., M. R. Rifkin, and D. J. L. Luck. 1977. Temperature sensitive mutations affecting flagellar assembly and function in *Chlamydomonas reinhardtii. J. Cell Biol.* 72:67–85.
Huang, B., G. Piperno, and D. J. L. Luck. 1979. Paralyzed flagella mutants of *Chlamydomonas reinhardtii* defective for axonemal doublet microtubule arms. *J. Biol. Chem.* 254:3091–3099.
Huang, B., G. Piperno, Z. Ramanis, and D. J. L. Luck. 1981. Radial spokes of *Chlamydomonas* flagella. Genetic analysis of assembly and function. *J. Cell Biol.* 88:80–88.
Huang, B., Z. Ramanis, S. K. Dutcher, and D. J. L. Luck. 1982*a*. Uniflagellar mutants of *Chlamydomonas*: evidence for the role of basal bodies in the transmission of positional information. *Cell.* 29:745–753.
Huang, B., Z. Ramanis, and D. J. L. Luck. 1982*b*. Suppressor mutations in *Chlamydomonas* reveal a regulatory mechanism for flagellar function. *Cell.* 28:115–124.
Kamiya, R. 1988. Mutations at twelve independent loci result in absence of outer dynein arms in *Chlamydomonas reinhardtii. J. Cell Biol.* 107:2253–2258.
Kamiya, R., E. Kurimoto, H. Sakakibara, and T. Okagaki. 1989. A genetic approach to the function of inner- and outer-arm dynein. *In* Cell Movement. Vol. 1. F. D. Warner, P. Satir, and I. R. Gibbons, editors. Alan R. Liss, Inc., New York. 209–218.
Kamiya, R., E. Kurimoto, and E. Muto. 1991. Two types of *Chlamydomonas* flagellar mutants missing different components of inner-arm dynein. *J. Cell Biol.* 112:441–447.
King, S. M., T. Otter, and G. B. Witman. 1986. Purification and characterization of *Chlamydomonas* flagellar dyneins. *Methods Enzymol.* 134:291–306.
Kurimoto, E., and R. Kamiya. 1991. Microtubule sliding in flagellar axonemes missing inner- or outer-arm dynein: velocity measurements on new types of mutants by an improved method. *Cell Motil. Cytoskeleton.* 19:275–281.
Laemmli, U. K. 1970. Cleavage of structural proteins during the assembly of the head of bacteriophage T4. *Nature.* 227:680–685.
Levine, R. P., and W. T. Ebersold. 1960. The genetics and cytology of *Chlamydomonas. Annu. Rev. Microbiol.* 14:197–216.
Loppes, R. 1969. A new class of arginine-requiring mutants in *Chlamydomonas reinhardi. Mol. & Gen. Genet.* 104:172–177.
Luck, D. J. L., and G. Piperno. 1989. Dynein arm mutants of *Chlamydomonas. In* Cell Movement. Vol. 1. F. D. Warner, P. Satir, and I. R. Gibbons, editors. Alan R. Liss, Inc., New York. 49–60.
Luck, D. J. L., G. Piperno, Z. Ramanis, and B. Huang. 1977. Flagellar mutants of *Chlamydomonas*: study of radial spoke-defective strains by dikaryon and revertant analysis. *Proc. Natl. Acad. Sci. USA.* 74:3456–3460.
Lux, F. G., and S. K. Dutcher. 1991. Genetic interactions at the *FLA10* locus: suppressors and synthetic phenotypes that affect the cell cycle and flagellar function in *Chlamydomonas reinhardtii. Genetics.* 128:549–561.
Mastronarde, D. N., E. T. O'Toole, K. L. McDonald, J. R. McIntosh, and M. E. Porter. 1992. Arrangement of inner dynein arms in wild-type and mutant flagella of *Chlamydomonas. J. Cell Biol.* 118:1145–1162.
McVittie, A. 1972*a*. Flagellar mutants of *Chlamydomonas reinhardii. J. Gen. Microbiol.* 71:525–540.
McVittie, A. 1972*b*. Genetic studies on flagellum mutants of *Chlamydomonas reinhardii. Genet. Res.* 19:157–164.
Mitchell, D. R., and J. L. Rosenbaum. 1985. A motile *Chlamydomonas* flagellar mutant that lacks outer dynein arms. *J. Cell Biol.* 100:1228–1234.
Mitchell, D. R., and Y. Yang. 1991. Identification of *oda6* as a *Chlamydomonas* dynein mutant by rescue with the wild-type gene. *J. Cell Biol.* 113:835–842.
Neville, D. M. 1972. Molecular weight determination of protein-dodecyl sulfate complexes by gel electrophoresis in a discontinuous buffer system. *J. Biol. Chem.* 246:6328–6334.
Piperno, G., and D. J. L. Luck. 1979. Axonemal adenosine triphosphatases from flagella of *Chlamydomonas reinhardtii. J. Biol. Chem.* 254:3084–3090.
Piperno, G., and Z. Ramanis. 1991. The proximal portion of *Chlamydomonas* flagella contains a distinct set of inner dynein arms. *J. Cell Biol.* 112: 701–709.
Piperno, G., Z. Ramanis, E. F. Smith, and W. S. Sale. 1990. Three distinct inner dynein arms in *Chlamydomonas* flagella. Molecular composition and location in the axoneme. *J. Cell Biol.* 110:379–389.
Porter, M. E., and K. A. Johnson. 1989. Dynein structure and function. *Annu. Rev. Cell Biol.* 5:119–151.
Sager, R., and S. Granick. 1953. Nutritional studies with *Chlamydomonas reinhardtii. Ann. NY Acad. Sci.* 466:18–30.
Smith, E. F., and W. S. Sale. 1991. Microtubule binding and translocation by inner dynein arm subtype I1. *Cell Motil. Cytoskeleton.* 18:258–268.
Waxman, L., and A. Goldberg. 1982. Protease La from *Escherichia coli* hydrolyzes ATP in a linked fashion. *Proc. Natl. Acad. Sci. USA.* 79:4883–4887.
Witman, G. B. 1986. Isolation of *Chlamydomonas* flagella and flagellar axonemes. *Methods Enzymol.* 134:280–290.
Witman, G. B., J. Plummer, and G. Sander. 1978. *Chlamydomonas* flagellar mutants lacking radial spokes and central tubules. *J. Cell Biol.* 76:729–747.